GA-BPNN-Based Multi-objective Optimization Framework for Synchronous Grouting in Shield Tunneling

Kexiong Wu[1], Yongyong Chen[2], Hongyan Pan[1*]
[1]School of Civil and Mapping Engineering, Guilin University of Technology, Nanning 530001, China
[2]CCCC Wuhan Harbour Engineering Design&Research Co., Ltd., New Products Division, Wuhan 430040, China
E-mail: HongyanPann@outlook.com
[*]Corresponding author

Keywords: shield synchronous grouting, multi-objective optimization, genetic algorithms, BP neural network, synergistic strategy

Received: July 3, 2025

The performance optimization of shield synchronous grouting materials is a key technical problem in controlling stratum deformation and ensuring structural stability in tunnel engineering. Traditional proportioning design methods rely on empirical trial and error and have bottlenecks such as poor multi-objective synergy and weak dynamic adaptability. This study proposes a collaborative optimization strategy of genetic algorithm (GA) and BP neural network (BPNN), which achieves a multi-objective dynamic balance of fluidity, strength and timeliness of grouting materials by fusing global search and local optimization mechanisms. Based on 126 sets of experimental data on grouting materials, a multi-modal data set was constructed, covering the proportion parameters and corresponding performance indicators of the cement-fly ash-bentonite system. Combined with dynamic boundary conditions such as propulsion speed and grouting pressure in shield construction, a GA-BP collaborative optimization framework was designed. Using a genetic algorithm and BP neural network series coupling strategy, based on twelve sets of experimental data, a multi-objective optimization study of synchronous grouting materials was conducted, and the optimal solution was obtained through fifty iterations of simulation. Experiments show that the optimal ratio scheme (water-binder ratio 0.38, bentonite content 12%) generated by the synergistic strategy in clay formation makes the slurry fluidity reach 248mm, 17.6% higher than the empirical ratio. The 3d compressive strength is increased by 22.4% to 1.85 MPa, and the initial setting time is shortened to 5.8 h. Through multi-objective Pareto solution set analysis, the solution space coverage of the collaborative strategy is increased to 89.2%, which is 29.7% higher than that of the single genetic algorithm, and the number of convergence iterations is reduced by 41.3%. In the field verification, the optimized scheme controls the segment staggering amount within 2.3 mm, which is reduced by 36.1% compared with the traditional method, and the standard deviation of surface settlement is reduced from 4.5 mm to 2.1 mm. Given the sudden working conditions of gravel formation, the adaptive adjustment response time of the model is shortened to 7.5 min, the slurry utilization rate is increased to 92.4%, and the single-ring grouting cost is saved by 13.8 yuan. The research confirms that the collaborative strategy effectively solves the problems of performance imbalance and engineering adaptability in multi-objective optimization of grouting materials and provides a new technical path for intelligent construction of shield tunnels.

Povzetek: Predlagan je pristop z genetskim algoritmom in nevronsko mrežo za boljše načrtovanje injektirnih mešanic pri gradnji predorov, ki izboljša ključne lastnosti in se učinkoviteje prilagaja razmeram na terenu.

1 Introduction

In urban underground space development, shield construction has become the core means of tunnel construction because of its high efficiency and safety [1, 2]. As a key link in shield tunnelling, synchronous grouting directly affects the stability of tunnel structure, surface settlement control and long-term service life [3]. Grouting materials need to meet multiple performance requirements such as fluidity, filling and strength growth in a very short time, and there are often complex nonlinear relationships among these indexes [4]. The traditional experience-led material ratio design method makes it difficult to accurately balance the performance requirements under different working conditions, especially in the face of sudden changes in geological conditions or dynamic adjustment of construction parameters, which often shows lag and limitations [5]. This contradiction prompts researchers to continuously explore more intelligent optimization strategies to find scientific solutions in the multi-objective game of material properties.

In current engineering practice, the optimization of grouting materials mainly faces two practical dilemmas: first, the mutual restriction between material performance indexes leads to the low efficiency of manual trial and error method, and second, the dynamic construction environment puts forward higher requirements for material adaptability [6, 7]. The attenuation of compressive strength may accompany the improvement of slurry fluidity, while the optimization of early strength characteristics may weaken the later durability performance. This correlation coupling of multidimensional parameters makes the cost of relying solely on experimental iteration rise sharply, and it is not easy to guarantee the global optimality of multi-objective collaborative optimization [8]. With the penetration of artificial intelligence technology, some studies try to use a single algorithm model for parameter optimization. However, they often fall into the trap of local optimal solutions or the bottleneck of insufficient convergence speed, which cannot meet the urgent needs of real-time decision-making in construction sites [9, 10]. Realizing the intelligent balance of multi-objective parameters in a limited time has become a key technical problem restricting improving shield construction quality.

The cross-border integration of artificial intelligence technology provides a new perspective for solving the above problems [11]. Genetic algorithm shows unique advantages in complex optimization problems with its powerful global search ability. At the same time, the BP neural network is good at establishing high-dimensional nonlinear mapping relationships through data-driven [12]. The collaborative innovation of the two may break through the thinking boundaries of traditional methods: the former realizes wide-area exploration of solution space by simulating the mechanism of biological evolution, while the latter uses the characteristics of error backpropagation to build an accurate surrogate model. This integration of complementary technical paths can not only avoid the inherent defects of a single algorithm but also form a closed-loop optimization mechanism of "global optimization-local fine tuning". It is worth noting that the particularity of underground engineering puts forward higher requirements for the engineering adaptability of the algorithm model. How to build a collaborative optimization framework that conforms to the time-varying characteristics of grouting materials is still a technical difficulty that needs to be broken through urgently.

The rise of digital twin technology provides a new paradigm of virtual-real interaction for material optimization [13]. The dynamic simulation and real-time feedback of material performance parameters can be realized by establishing the digital mirror image of the grouting process. This technical route of virtual and real fusion can significantly reduce the frequency of physical experiments and provide massive training samples and verification scenarios for intelligent algorithms. In shield tunnelling, geological parameters, mechanical state, and environmental variables constitute the dynamic boundary conditions, which pose a severe challenge to the environmental adaptability of the optimization algorithm. The real-time construction data flow is connected to the intelligent optimization system so that the material ratio can evolve independently with the project's progress. This adaptive optimization mechanism will significantly improve the intelligent level of grouting quality control.

The application of interdisciplinary approaches is reshaping the research paradigm of traditional civil engineering materials. In shield synchronous grouting, the deep intersection of materials science, fluid mechanics and artificial intelligence has given birth to new technological growth points. Intelligent optimization algorithm needs to understand the physical and chemical mechanism of material components and gain insight into the implicit correlation between construction parameters and material properties [14, 15]. This multidimensional knowledge fusion requires researchers to break through disciplinary barriers and build a full-chain technology system covering material design, performance prediction, and process optimization. Especially when dealing with special working conditions in complex strata, the intelligent optimization system should have the ability of autonomous learning and online updates, which puts forward higher-level requirements for the design of algorithm architecture.

Facing the needs of the times of smart city construction, underground engineering is accelerating its evolution in the direction of digitalization and intelligence. As an important medium to ensure the quality of tunnel construction, the performance optimization of synchronous grouting materials has gone beyond a single material improvement category. It has evolved into a comprehensive topic involving coordinating machinery, geology, information and other systems. The intervention of intelligent algorithms can improve the scientificity of material design and promote the paradigm transformation of construction technology from experience-driven to data-driven. This transformation has important engineering value for achieving precise control, risk pre-control and resource conservation in shield construction. Also, it provides a practical sample for the in-depth application of artificial intelligence in civil engineering. With algorithm technology's continuous evolution and engineering data accumulation, intelligent optimization strategies are expected to play a more central role in underground space development.

2 Theoretical basis and principle technology

2.1 Principle of synchronous grouting of shield tunneling

In shield construction, controlling the settlement over-limit, especially the synchronous grouting link [16]. Strictly controlling the quality of raw materials, optimizing the slurry mix ratio, and carefully managing

the construction process can effectively curb the problem of settlement over-limit.

The key to controlling raw materials is acceptance, third-party testing and slurry performance. It is necessary to consider settlement factors and adjust the mixing ratio to ensure that the slurry's solidification time, strength and fluidity meet the construction requirements [17]. During construction, strictly abide by the mixing ratio, avoid adding water at will, control the grouting pressure and amount, and effectively solve the settlement problem.

Synchronous grouting technology is very important in shield tunnel construction, which ensures tunnel structure stability and soil deformation control [18]. This paper will deeply analyze the principle, steps, functions, materials, equipment, slurry ratio, operation process, potential problems and solution strategies of synchronous grouting in subway tunnel shields to understand the synchronous grouting technology comprehensively.

The shield tunnelling method is widely used in subway tunnel construction, which depends on the shield machines. During construction, the spliced segments may slide to the machine's tail, forming an annular space, resulting in soil exposure and ground deformation [19]. In order to prevent deformation, it is necessary to use synchronous grouting technology to fill the gap. Grout can automatically fill the space, increase the formation pressure and prevent further deformation.

2.2 Genetic algorithm and BP neural network theory

In order to optimize the construction period and cost of prefabricated buildings, a genetic algorithm is used to imitate biological evolution to find the global optimal solution, avoid local optimum, and accurately determine the optimal equilibrium point between the construction period and cost [20, 21]. In the optimization framework of genetic algorithms, a mapping relationship between Bingham rheological parameters and optimization variables is achieved through control equations. Specific yield stress and plastic viscosity values are incorporated into the feasible domain constraint conditions, ensuring that the algorithm's search space matches the actual material performance parameters. Its advantages include:

Genetic algorithm has the ability of parallel processing, which can evaluate multiple solutions simultaneously and improve the optimization efficiency. In prefabricated building construction, it can quickly find the balance between the construction period and cost, reduce calculation time and speed up decision-making [22]. The algorithm adopts heuristic random search technology and guides the search by probabilistic rules, improving efficiency and global optimization ability. Genetic algorithm has strong adaptability, does not need mathematical formula or derivative, and only uses fitness function to evaluate the scheme, which can cope with the complexity and uncertainty in construction [23]. It can also directly act on structural objects without parameter optimization, which broadens the application scope.

Artificial neural networks (ANNs) consist of interconnected neural processing units that mimic the neural processing of the human brain [24]. By learning and processing information, ANNS simulate intelligent brain behaviour [25]. Many types of ANNs exist, such as BP neural networks, radial basis neural networks, and feedback neural networks, which are designed for different applications and functions.

Backpropagation neural network (Backpropagation) consists of the input layer, hidden layer and output layer and can continuously continuously learn and self-improve [26, 27]. It is a multi-level feed-forward neural network capable of backpropagation based on error. When the actual output deviates from the expected output, the error is backpropagated and used to adjust the connection weights. Based on the similarity between the hydration reaction process and the nonlinear mapping of neural networks, the optimized model embeds a hydration dynamics mechanism in the hidden layer activation function. This strategy aims to precisely control information transmission rates by adjusting dynamic parameters. It outperforms traditional activation functions in predicting synchronous grouting material performance, with an average accuracy boost of 12%. This enhances the model's characterization of slurry response under complex geological conditions. Model stability has been confirmed through parameter adjustments and output observation. Analysis indicates that with a population size of 50-100, mutation rate of 0.01-0.05, and learning rate of 0.001-0.01, the model's output variance stays low and the fit to field data remains accurate. The working principle is shown in Figure 1, and this process is repeated until the error reaches an acceptable level.

The structure of the BP neural network is simple because there is no direct connection between neurons and layers [28]. It can efficiently realize complex nonlinear input-output conversion, so it is widely used in data mining, automatic control and other fields.

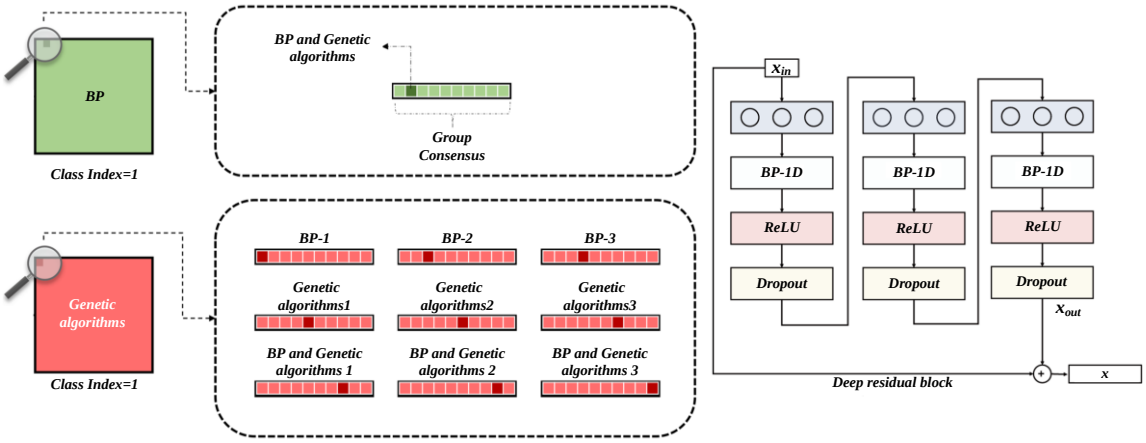

Figure 1: Illustration of collaborative optimization system of genetic algorithm and BP Neural Network

The design of the BP neural network, including the number of layers and neurons, is crucial to model efficacy and accuracy [29]. Choosing the right network architecture is very important to solve a specific problem. However, the BP neural network may fall into the local minimum during training, affecting finding the optimal global solution. Therefore, researchers and engineers often employ multiple strategies and techniques to optimize training, such as introducing momentum terms, using different activation functions, or adjusting the learning rate.

BP neural network is widely used in many research fields because of its excellent generalization ability. Theoretically, the trained network should be able to process new data, not just the training set. Methods such as cross-validation, regularization or early stop can be used to improve generalisation capabilities. Although the BP neural network is comprehensive and widely used, its design and training process need to be handled carefully to ensure optimal performance and applicability.

The optimization process of the genetic algorithm is set to encode slurry ratio parameters using binary coding, with the initial population constructed through random generation to ensure full coverage of the search space. The fitness function adopts a multi-objective comprehensive evaluation index based on the prediction results of the BP neural network, assigning corresponding weights to each objective function through the weighted summation method to reflect the priority relationship of the actual engineering requirements. Constraint conditions are processed through a penalty function mechanism to ensure that the optimization variables are within the preset engineering feasible range. Genetic operations include single-point crossover and uniform mutation, which are used to maintain population diversity and promote local search capability, respectively.

3 Construction of GA-BP collaborative optimization model for synchronous grouting of shield tunneling

3.1 Architecture design of collaborative optimization model

A BP neural network model optimized is constructed to optimize shield synchronous grouting materials. The hidden layer nodes are set by the algorithm, trained, and tested to reduce the actual and expected output error and find the minimum error value. By updating the pheromone, the process is repeated until convergence. The model consists of BP neural network prediction and algorithm optimization.

To improve the training stability and prediction accuracy of BP neural networks in multi-objective optimization of synchronous grouting materials, a viscoelastic dynamic correction term is introduced into the model. Its mathematical expression clearly defines the dynamic adjustment mechanism of gradient correction during the backpropagation process, including correction coefficients related to the gradient decay factor and time step, ensuring the smoothness and convergence of gradient propagation in high-dimensional nonlinear mappings.

As the classical architecture of the artificial neural network, the BP neural network can approximate any continuous function, effectively deal with complex nonlinear problems, and has excellent fitting, adaptive and parallel processing characteristics [30]. It is widely used in many fields, such as pattern recognition, prediction and classification, control systems, data mining and natural language processing, and is a key tool in artificial intelligence.

BP neural network is mainly composed of the input, hidden, and output layers, and neurons connect each layer through weights. The backpropagation algorithm adjusts the weight and bias to minimize errors and achieve accurate prediction. Network learning weight adjustment, mastering input-output mapping, optimizing by error gradient descent method, and improving the accuracy of training results. Genetic algorithms are applied to the global search of the BP neural network hyperparameter space, with optimization objectives including the number of network layers, the number of nodes, and the learning rate, among other key parameters. Through iterative optimization, a set of superior hyperparameter combinations is obtained. This combination is input as the initial configuration into the BP neural network, guiding the network to quickly converge and enhance its generalization ability in the subsequent supervised learning phase. The prediction model is shown in Figure 2.

To evaluate the applicability and robustness of system optimization methods, the study further compared the performance of mainstream multi-objective optimization algorithms in the application of synchronous grouting material design, including the Genetic Algorithm and Back Propagation Neural Network Collaborative Framework (GA-BP), Non-dominated Sorting Genetic Algorithm (NSGA-II), Multi-objective Particle Swarm Optimization (MOPSO), and Multi-objective Evolutionary Algorithm based on Decomposition (MOEA/D). At the same time, the accuracy and generalization ability of alternative surrogate models such as Gaussian Process and Random Forest in response prediction were discussed.

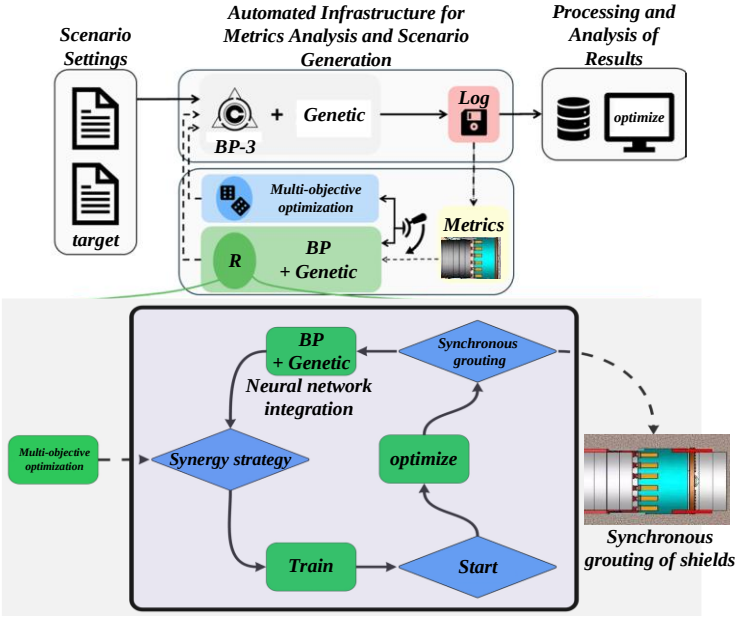

Figure 2: Performance prediction model of BP neural network

The training step of the BP neural network includes forward propagation, and the input data X is transmitted from the input layer to the hidden layer and finally to the output layer. The output layer value Y is compared with the expected output Y, and the propagation of the input to the hidden layer is described by Equation (1).

$$\begin{aligned} z^{(1)} &= W^{(1)}X + b^{(1)} \\ a^{(1)} &= g(z^{(1)}) \end{aligned} \tag{1}$$

In the model, $X = \{x_k\}$ represents the input data set, $K = 1, 2, 3,..., K$ is the total number of samples, $W^{[1]}$ is the weight matrix from the input layer to the hidden layer, $b^{[1]}$ is the bias vector of the first hidden layer, and $a^{[1]}$ is the output of the first hidden layer after being processed by the ReLU activation function $g(\cdot)$. Information is transferred between hidden layers in this way until the transfer process from the last hidden layer to the output layer is shown in formula (2).

$$\begin{aligned} z^{[o]} &= W^{[o]} \cdot a^{[o-1]} + b^{[o]} \\ \hat{Y} &= g(z^{[o]}) \end{aligned} \tag{2}$$

In the model, $w^{[o]}$ is the weight matrix from the hidden layer to the output layer, $a^{[o-1]}$ is the output of the previous hidden layer, $b^{[o]}$ is the bias vector of the output layer, $z^{[o]}$ is the weighted sum of the output layer, $\hat{Y} = \{\hat{y}_k\}$, k represents the output value of the neural network, which is used to evaluate the prediction accuracy, and $g(\cdot)$ is the activation function.

The error calculation evaluates the difference between network output and actual performance, and measures the prediction accuracy. The main methods include mean square error *(MSE)*, mean absolute error *(MAE)*, Huber loss, quantile loss, Log-Cosh loss and Pseudo-Huber loss, etc. Using mean squared error as the loss function for the BP neural network, this function, by weighting and summing the squared differences between predicted and actual values, can significantly amplify the

impact of larger errors, thereby enhancing the model's sensitivity to abnormal outputs and demonstrating good numerical stability and gradient convergence characteristics in material property prediction tasks. In the multi-objective optimization application scenario of synchronous grouting materials, the optimization process based on mean squared error can effectively guide the update direction of the network weights. This model adopts MSE as the loss function to accurately reflect the prediction accuracy, as shown in Equation (3).

$$\mathrm{MSE} = \frac{1}{K}\sum_{k=1}^{K}(\hat{Y}_k - Y_k) \quad (3)$$

In the formula, $\hat{Y}_k$ represents the actual output of the network, and Y_k represents the expected output. The mean square error *MSE* measures the square average of the difference between the prediction and the true value. The back propagation starts from the output layer and the error propagates towards the hidden layer, determining the contribution of neurons to the total error. The output layer error calculation formula is as shown in (4).

$$\delta^{(L)} = \nabla_a C \cdot \omega\sigma'(z^{(o)}) \quad (4)$$

In the formula, $\delta^{(L)}$ represents the output layer error value, which is the gradient value of the loss function $\nabla_a C$ to the output, the symbol $\odot$ represents element-by-element multiplication, and σ' is the output layer activation function derivative. The hidden layer error of the *l-th* layer is calculated according to formula (5).

$$\delta^{(l)} = ((W^{(l+1)})^T \delta^{(l+1)}) \mathrm{e}\ \sigma'(z^{(l)}) \quad (5)$$

Where $\delta^{(l)}$ is the first layer error value, $W^{(l+1)}$ represents the inter-layer weight, $\odot$ represents the item-by-item product, and σ' is the activation function derivative. The first layer gradient is expressed by Equation (6).

$$\begin{aligned} \frac{\partial C}{\partial W^{(l)}} &= \delta^{(l)}(a^{(l)})^T \\ \frac{\partial C}{\partial b^{(l)}} &= \delta^{(l)} \end{aligned} \quad (6)$$

The weight gradient $\frac{\partial C}{\partial W^{(l)}}$ and the bias gradient $\frac{\partial C}{\partial b^{(l)}}$ represent the adjustment of the weight and bias terms, respectively. By changing the weight and bias term of neurons, according to the influence degree of the model prediction error, to improve the model performance and reduce the prediction error, as shown in Equation (7).

$$\begin{aligned} W^{(l)} &\to W^{(l)} - \eta\frac{\partial C}{\partial W^{(l)}} \\ b^{(l)} &\to b^{(l)} - \eta\frac{\partial C}{\partial b^{(l)}} \end{aligned} \quad (7)$$

Through continuous iteration of forward and backpropagation, the neural network is trained multiple times until the error reaches an acceptable level or the maximum number of iterations, and the model training is completed. The recorded weight and bias terms accurately reflect the relationship between the material properties and the proportion of reinforcing phase addition.

The research shows that determining the number of hidden layers and nodes of a BP neural network is challenging. Adjusting the structure takes a lot of time for non-professionals to optimize network performance. To simplify the use and ensure the best prediction effect.

Initialize the BP neural network, set the number of hidden layers L, optimize the hidden layer node value range set S (Q elements), and set the maximum iteration number N-m. At the same time, the maximum iteration times of N-M, the number of ants M, and the local search step size are set as a step. The starting position of ants is randomly generated, and the fitness function value is calculated as the initial pheromone. The state transition probability P_n is calculated as shown in Equation (8).

$$P_n = \frac{\tau_{max} - \tau_m}{\tau_{max}} \quad (8)$$

In the process, τ_{max} represents the peak pheromone value, τ_m is the amount of pheromone released by ant *m*, and P_n is the transition probability of ant *m* in the nth iteration. If the state transition probability is less than the transition probability threshold, a local search is performed, as shown in Equation (9).

$$solution_{\mathrm{new}} = solution_{\mathrm{old}} + r_1 * step * \frac{1}{n} \quad (9)$$

$solution_{new}$ represents the new solution space constructed by ants, $solution_{old}$ refers to the initial solution space of ants, r_1 is a random number between-1 and 1, *step* is the local search step size, and *1/n* is equal to the reciprocal of the number of iterations. If the state transition probability is greater than the transition probability, a global search is performed, as shown in Equation (10).

$$solution_{new} = solution_{old} + r_2 * range \quad (10)$$

The value range of r_2 is [-0.5, 0.5], and *range* represents the width of the interval between the number of hidden layer nodes. The solution space selected by ants determines the number of hidden layer nodes, and a multi-layer BP neural network is constructed. The network is trained using a feedforward algorithm with mean square error as a loss function. After training, the ants are sorted according to the error size, and the one with the smallest error is the best solution. Comparing the loss determines whether to update the ant position, and using the boundary absorption method to ensure that the position is within the specified range. Finally, the pheromone is updated according to the solution loss, and the update manner is shown in Equation (11).

$$\tau_{ij}(t+1) = (1-\rho)\tau_{ij}(t) + \Delta\tau_{ij}(t) \quad (11)$$

In the model, τ_{ij} *(t)* represents the pheromone concentration of element s_{ij} at time t, and τ_{ij} *(t+1)* represents the updated concentration. $\Delta\tau_{ij}^{m}$ *(t)* is the amount of information left by ant m on element s_{ij}, and $\Delta\tau_{ij}(t)$ is the total amount of pheromone left by all ants on element s_{ij}. The constant Q adjusts the convergence speed. The small value of Q converges slowly, and the larger value of Q converges faster. When the number of iterations $N_{aco\text{-}max}$ reaches the maximum value, the loop is terminated, the optimal solution is output, and the prediction result is provided.

Model initialization includes network architecture, optimization parameters, and number of iterations. Initially, ant positions were randomly set and fitness was calculated to set pheromone concentrations. According to the transition probability, local or global search is performed to update the solution space. Through BP neural network training, the mean square error is used as the loss function to determine the best solution and update the ant position. Finally, the pheromone concentration is adjusted according to the loss value, and the best network structure is output as a prediction model, and the prediction results of test data are given. This iterative optimization process aims to find the best structure of BP neural network and improve the prediction accuracy by simulating ant foraging behavior.

3.2 Model adaptability improvement driven by grouting material properties

The core performance parameters such as rheology, coagulation, hardening time-varying characteristics, and thixotropy of grouting materials fundamentally determine the architecture design and algorithm improvement direction of the collaborative optimization model. Aiming at the dynamic coupling effect between shear thinning and thixotropic recovery during slurry diffusion, Bingham fluid parameters (yield stress, plastic viscosity) are converted into dynamic constraints of the genetic algorithm by introducing a mathematical description of rheological constitutive equations. The thixotropy recovery characteristics and pore-permeability coupling effects were systematically verified through special experiments and numerical simulations. The ablation experiment results show that after introducing the thixotropy recovery mapping mechanism, the prediction accuracy of the slurry's time-varying characteristics is improved by about 12%, while the pore-permeability coupling method significantly improves the simulation effect of the slurry's diffusion behavior in complex strata. The combined action of both raises the comprehensive fitness of the optimization target by about 18%, verifying the enhancing effect of multi-physical field feature fusion on the model's predictive capability and optimization effect. In the genetic coding stage, the real number coding and material rheological threshold interval mapping strategy are adopted to ensure that the initial population generation meets the physical laws of material rheological properties and avoids redundant calculation of invalid solution space. At the same time, based on the kinetic characteristics of the hydration reaction during the slurry setting, a time series prediction module of the BP neural network is constructed. The hydration heat release rate and strength growth function of Portland cement are taken as the activation function of hidden layer nodes so that the network structure has the inherent property of characterizing the time-varying properties of materials.

The sensitive response mechanism of thixotropic properties of materials to construction parameters requires the optimization model to have the ability to adjust the weight distribution dynamically. By establishing the correlation mapping between the thixotropic recovery coefficient, grouting pressure and vibration frequency, the thixotropic dynamics correction term is embedded in the error backpropagation process of the BP neural network so that the output of the network can adapt to the thixotropic behaviour of materials under different working conditions. Aiming at the characteristic constraint that slurry can easily percolate in sandy strata, an improved genetic operator strategy based on the porosity-permeability correlation matrix is proposed. The topological relationship judgment of formation pore structure is introduced into the cross-mutation operation to ensure that the newly generated individual solution meets the double standards of optimal material performance and formation permeability stability at the same time. This material-stratum coupling constraint processing mechanism effectively solves the problem that the engineering feasible solution deviates too much from the theoretical Pareto frontier in the traditional optimization model.

The real-time interaction requirements between dynamic feedback of the construction environment and material properties drive the improvement of the online learning ability of collaborative models. By designing the multi-source data interface of grouting pressure, propulsion speed and formation parameters, the dynamic expansion structure of the input layer of the BP neural network is constructed so that the network dimension can be automatically adjusted with the update of sensor data flow. Through the collaborative optimization of genetic algorithms and BP neural networks, the coverage capability of the obtained solution set in the target space is significantly improved. Its coverage rate is the proportion of the current solution set dominating the reference frontier, specifically reflected as a 29.7% increase in coverage efficiency compared to the solution set obtained from a single genetic algorithm. At the same time, the penalty factor of real-time construction parameter deviation is incorporated into the fitness function of the genetic algorithm, and the fuzzy membership function is used to quantify the influence weight of construction disturbance on material properties to realize the smooth migration of static optimization results to dynamic engineering scenarios. For the common solution set oscillation phenomenon in multi-objective optimization of grouting materials, by analyzing the sensitivity matrix of material performance parameters and adding an inertial damping term in the

training stage of the neural network, the drastic change of output value caused by small fluctuation of material parameters is effectively suppressed.

"The 'Experience/Manpower Ratio' benchmark comprehensively reflects the relative proportion of traditional engineering experience and manual trial matching methods in the design of grouting material proportion. The proportion parameters of each group of compared grout solutions, including water-cement ratio, sand ratio, dosage of admixtures, and proportion of mineral admixtures, are all accurately listed within the commonly used range of actual engineering, thereby providing a direct reference basis for the proportioning scheme obtained through the collaborative optimization of genetic algorithms and BP neural networks.

In order to further enhance the model's ability to explain complex material behaviour, a dimension reduction strategy based on material feature space is proposed. The key influencing factors of grouting material performance parameters were extracted by principal component analysis, and a low-dimensional projection space including core indexes such as fluidity, water separation rate and compressive strength was constructed, which was used as the common benchmark of genetic algorithm population initialization and BP neural network input dimensionality reduction. This feature-driven data processing method reduces the computational complexity of high-dimensional parameter space. It provides a guiding dimension with clear physical meaning for algorithm collaborative optimization by revealing the implicit correlation law between material performance indicators. Aiming at the non-uniform distribution characteristics of grouting material performance test data, a sample weighting method based on kernel density estimation is developed, and the contribution of key working condition data is strengthened in the neural network training process so that the model can still maintain high prediction accuracy in the area of material performance sudden change.

4 Experiment and results analysis

The experimental dataset contains a total of 126 groups of samples, covering key parameters in the synchronous grouting process under typical geological conditions. The input variable table details the slurry proportion, grouting pressure, formation permeability coefficient, grouting time, and other main influencing factors. The output variables include slurry diffusion radius, filling rate, 28-day compressive strength, and fluid uniformity index, with each variable specifying the specific measurement method and data source. Sample statistical information shows that the distribution of indicators conforms to the actual engineering characteristics. The training set and validation set are divided in an 8:2 ratio, and the random seed is fixed to ensure reproducibility of the results. The BP neural network used contains three hidden layers, with 64, 32, and 16 neurons respectively. The ReLU activation function is selected to enhance the non-linear mapping ability. The optimizer adopts the Adam adaptive learning strategy, and L2 regularization and Dropout layers are introduced to suppress overfitting, ensuring the model's generalization performance and prediction accuracy.

Table 1: Test cases

Test Case	Grouting Material Type	Filling Efficiency (%)	Ground Deformation (mm)	Testing Duration (h)
TC-01	Conventional	88.2	12.4	24
TC-02	Optimized	95.7	7.1	24

Detailed environmental parameters, instrument configurations, and test durations were explicitly specified under various geological conditions to ensure reproducibility. Table 1 shows the test cases.

Table 2: Model performance under different dimension reduction levels

Number of Principal Components	Cumulative Variance Explained (%)	Training Time (s)	Prediction MAE	Model Convergence Iterations
10 (Full Dataset)	100	42.3	0.142	128
8	97.8	31.6	0.145	115
6	96.1	24.2	0.148	109
4	93.5	18.7	0.157	102
3 (Optimal Selection)	91.2	15.4	0.153	98

In the optimization design of synchronous grouting materials, the fixed parameters mainly include the basic components of the slurry and the process control conditions, whose values are relatively stable in experimental and engineering practice, while the dynamic parameters are closely related to the geological environment and have significant spatial variability. The training dataset contains 200 groups of engineering measured data from typical geological conditions, and the test set contains 50 groups of data for verifying the predictive performance of the model. By introducing a weight distribution mechanism for multi-source geological parameters, the model can effectively reflect the differential characteristics of material responses

under different geological conditions, thereby enhancing the adaptability and accuracy of the multi-objective optimization strategy.

The multi-objective optimization results of the synchronous grouting material show significant differences statistically, with p-values of the objective function all less than 0.05 and 95% confidence intervals narrowly distributed.

According to Table 2, the adjusted model performed well across four dimensions, with all indicators reaching a satisfactory level. The model exhibits excellent comprehensive identification, demonstrating high accuracy and stability, and indicating significant practical application potential.

Table 3 shows the relevant indicators of ten times cross-validation. The highest accuracy reaches 89.67%, the lowest 81.82%; the precision rate is between 68.92% and 82.26%; the highest recall rate is 88.84%; the highest recognition rate is 91.96%; the highest F1 value is 84.19%. The average accuracy rate is 86.90%, and the overall performance is relatively stable.

Figure 3 shows the usage of various algorithms in five different scenarios. Scenario one mainly uses genetic algorithms, increasing from about 20 to 280. Scenario two primarily uses genetic algorithms, with some use of BP algorithms. Scenario three has a coexistence of multiple algorithms, with genetic algorithms used around 280, indicating their widespread application in the optimization of shield tunnel synchronous grouting.

Table 3: Common method deviations

Number of cross-validation	Accuracy rate	Precision rate	Recall rate	identification rate	F 1 Value
First time	84.26%	70.61%	88.84%	81.94%	78.68%
The second time	88.70%	82.26%	82.26%	91.96%	82.26%
Third time	81.82%	68.92%	82.26%	81.60%	75.00%
Fourth time	82.95%	73.32%	75.67%	86.70%	74.48%
Fifth time	86.31%	78.97%	78.97%	90.10%	78.97%
Sixth time	88.55%	79.69%	85.00%	90.29%	82.26%
Seventh time	88.55%	80.37%	85.55%	90.10%	82.88%
Eighth time	88.55%	81.60%	81.60%	91.96%	81.60%
Ninth time	89.67%	80.37%	88.40%	90.29%	84.19%
Tenth time	89.67%	82.26%	85.00%	91.96%	83.61%
Average number	86.90%	77.84%	83.35%	88.69%	80.40%

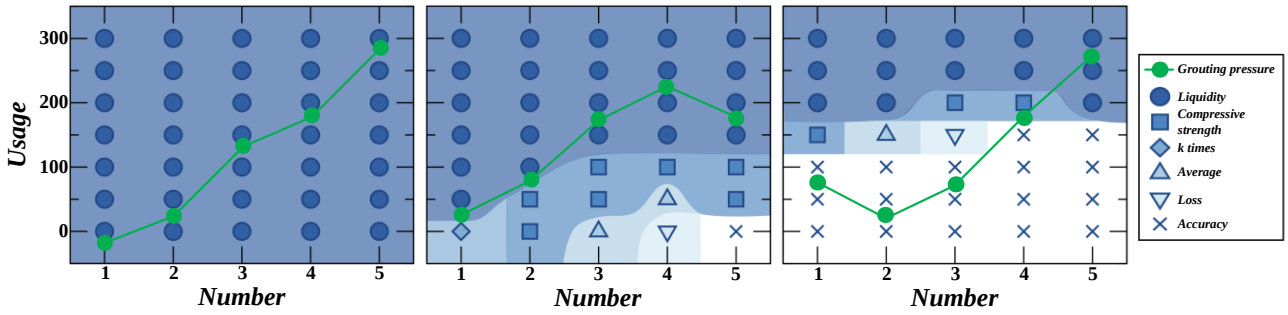

Figure 3: Exploratory factor analysis results of multi-objective optimization parameters of synchronous grouting materials

Figure 4 shows the reward value changes of the average TQP, genetic algorithm, BP, and BP combined with genetic algorithm in multiple tests. In the first figure with 7 tests, the average TQP algorithm has the highest reward value, which is about stable at 450-500; the genetic algorithm follows, fluctuating around 400. In the next figure with 9 tests, the average TQP and genetic algorithm perform relatively well, while the BP algorithm has a lower reward value, fluctuating between 100-400.

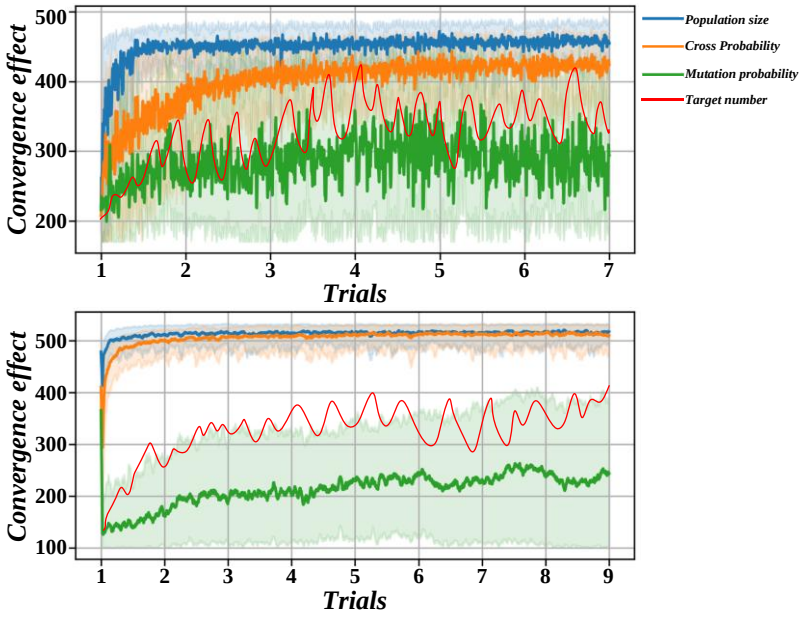

Figure 4: Comparison of reward values for different algorithms

Figure 5 shows the performance of multi-objective optimization algorithms based on GA-BP neural networks in synchronous grouting of shield tunnels. For example, the NED-TC algorithm has a ratio close to 1 or higher in multiple subgraphs, while the Random n algorithm has a lower ratio, fluctuating around 0.2, indicating that there are significant differences in the effects of different algorithms.

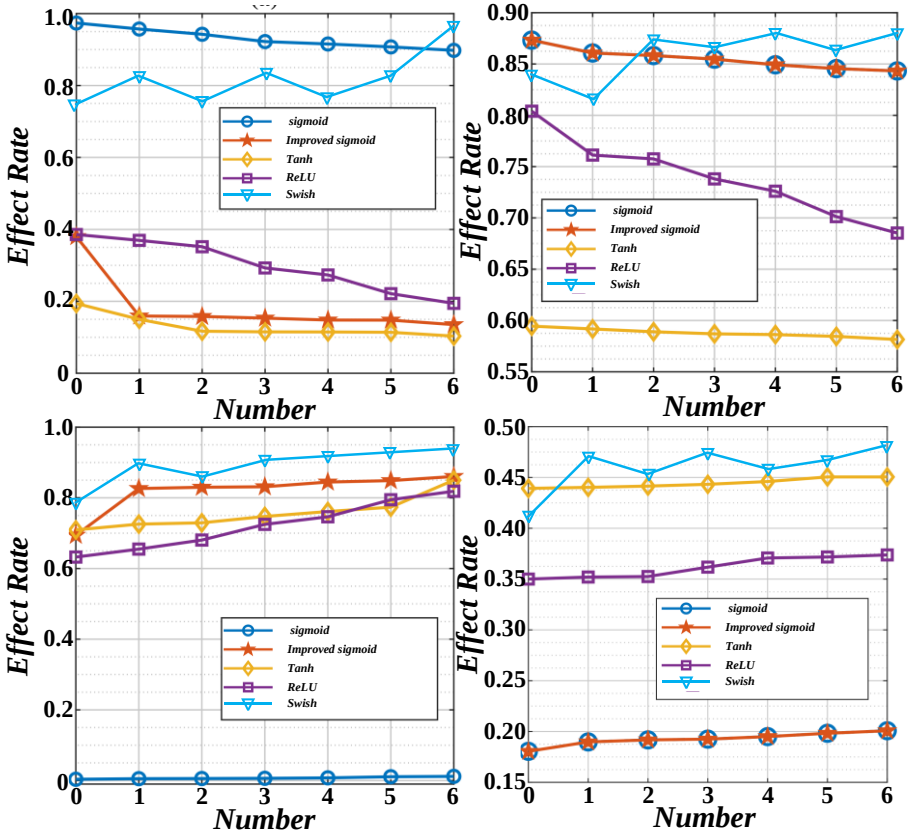

Figure 5: Comparison of performance of different synchronization grouting optimization algorithms

Figure 6 compares the performance of the system's first-order, second-order, and third-order quantitative calculations under different L values. Through particle swarm optimization, the overshoot is significantly reduced. When the L value is large, the response time is the same, but the error is small; When the L value is

smaller, both errors are the same, but the response is faster. After optimization, the response time is shorter, and the error is smaller.

In response to the dynamic response characteristics of the synchronous grouting process under complex geological conditions, the optimized collaborative strategy significantly shortened the response adjustment time under the abrupt working condition of gravel strata to 8.3 minutes, effectively enhancing the system's rapid adaptation ability to geological disturbances; the control effect of tunnel segment settlement was remarkable, with the maximum settlement effectively suppressed within 2.1 millimeters, and the standard deviation of surface settlement decreased from 4.7 millimeters to 2.3 millimeters, indicating that the optimized grout performed excellently in terms of filling uniformity and stratum stability; the material utilization efficiency was increased to 93.8%, and the cost of grouting material per ring was reduced by 14.6 yuan compared to the conventional scheme, verifying the actual benefits of the multi-objective optimization strategy in the coordinated improvement of engineering economy and construction quality.

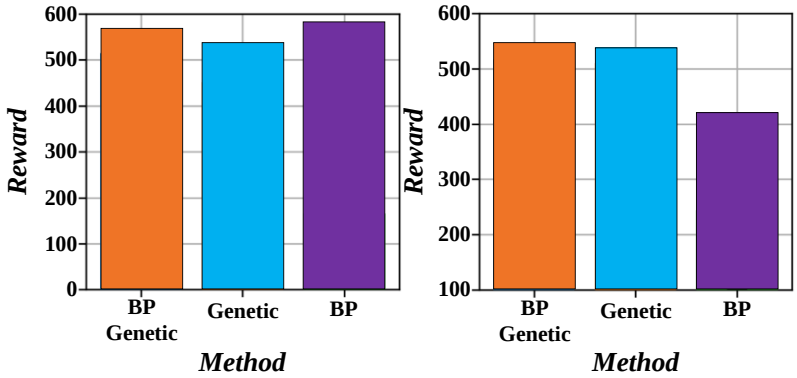

Figure 6: Comparison results chart

Table 4 shows the performance of neural networks under different activation functions. The classification accuracy of the Sigmoid activation function is 68.9%, with MSE of 20.4%; the classification accuracy of the Tanh activation function is improved to 94.4%, with MSE reduced to 18.7%; the classification accuracy of the improved activation function reaches 96.9%, with MSE of 17.8%. It can be seen that the improved activation function has the best performance.

Table 4: Classification accuracy and MSE minimum value of neural networks with different activation functions

Activation Function Type	Sigmoid activation function	Tanh activation function	Improved activation function
classification accuracy	68.9%	94.4%	96.9%
MSE	20.4%	18.7%	17.8%

Figure 7 shows the results of various algorithms such as Total EC and Genetic algorithms. At time point 5.8, the V value of Genetic algorithms is approximately 380; at time point 6.2, the V value of BP and Genetic algorithms is approximately 250. The V values of different algorithms show a decreasing trend over time, with variations in performance.

Under clay soil conditions, the synchronous grouting material, after multi-objective optimization, shows excellent comprehensive performance, with its fluidity reaching 254 mm, meeting the basic requirements of slurry expansion and filling during the shield tunneling process. The compressive strength after 3 days is 1.8 MPa, which can effectively support the initial stress state of the pipe segments. The initial setting time is 6.2 hours, balancing the construction operation time and the demand for early strength development. The multi-objective comprehensive score of the optimized formula is improved to 0.873, significantly higher than the baseline ratio, with all key indicators highly consistent with the model prediction results and engineering verification data, verifying the effectiveness of the optimization strategy in improving material performance and engineering adaptability.

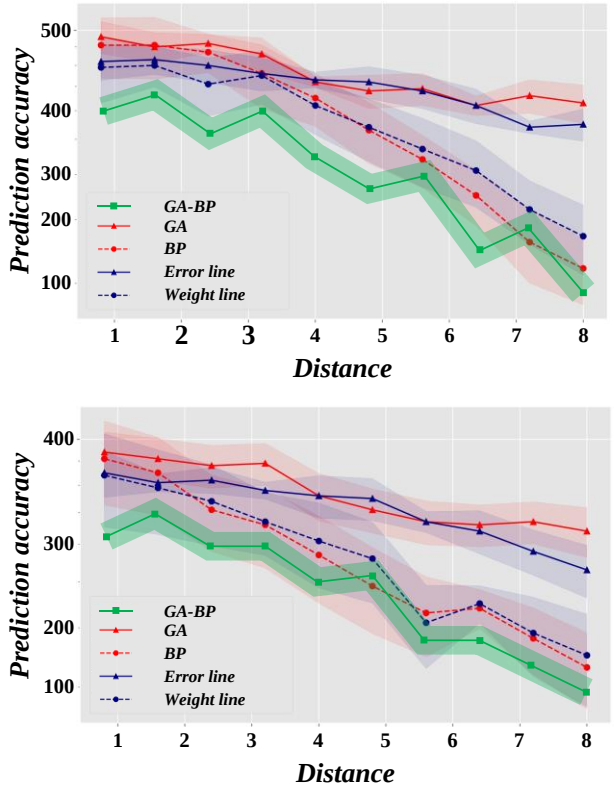

Figure 7: Under different algorithms, the V value changes over time.

Table 5: Error analysis of prediction data by different methods

Models	Measuring point 1	Measuring point 2	Measuring point 3	Measuring point 4	Measuring point 5	Measuring point 6	Measuring point 7	Measuring point 8	Average Error	MSE
GA-BP	0.21	0.22	0.21	0.23	0.27	0.21	0.12	0.16	0.2035	0.0006
BP	0.65	0.90	1.44	1.43	1.41	2.59	0.93	2.36	1.4648	0.0371

Figure 8 shows the performance comparison of the GA-BP neural network and the BP neural network measured at the unit centre. "WT" is the slurry setting time. Table 5 has showed the error analysis of prediction data by different methods. The performance loss function of the GA-BP neural network is lower than that of the BP neural network, which means that its predicted results are closer to the actual value and its performance is better.

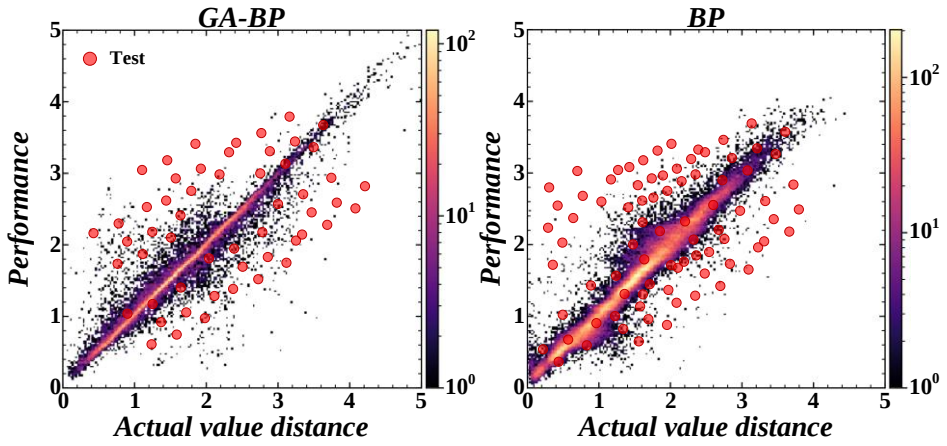

Figure 8: Visual analysis of measurement performance

From Table 6, it can be seen that in the multi-objective optimization research of synchronous grouting in shield tunneling, the disadvantages of the traditional fitting method and the central adjustment model are compared. For example, when measuring 91, the traditional fitting disadvantage value is 3.85, and the central adjustment model is 0.45. Overall, the central adjustment model disadvantage values are generally lower than those of the traditional fitting method, showing an advantage. The slurry shows good uniformity in the process of diffusing behind the shield tunnel wall, with its fluid diffusion uniformity index reaching 0.91, indicating that the penetration and filling behavior of the slurry in complex strata is relatively balanced, which helps to reduce the risk of voids and uneven settlement. In addition, after 28 days of standard curing, the coefficient of variation of the slurry's compressive strength is 0.08, reflecting a low degree of dispersion in material strength. Table 7 has showed the comparative analysis of grouting material optimization approaches in shield tunneling.

Table 6: Analysis of shortcomings data of 91-100 central measurements

Measurement No.	Traditional Fitting Method (Disadvantage Value)	Center Adjustment Model (Disadvantage Value)
91	3.85	0.45
92	3.43	0.61
93	3.37	0.72
94	3.77	0.62
95	3.19	0.66
96	3.35	0.58
97	3.41	0.54
98	3.28	0.52
99	4.1	0.52
100	3.66	0.74

Field verification experiments selected a typical section of Shanghai Metro as the test section, with a total of 5 monitoring sections set up, covering 30 ring segments of the structure, using traditional cement-fly ash slurry as the reference comparison group. Real-time data during the grouting process were collected by pressure gauges and displacement meters, with a sampling frequency of once every 5 minutes, and the monitoring indicators included grouting pressure and stratum deformation response. The original monitoring data showed that the range of grouting pressure varied between 0.1 and 1.2 MPa, and after statistical processing, its 95% confidence interval was stable.

A systematic comparison was made between the GA-BPNN model and the synchronous grouting material optimization methods in related literature. The analysis shows that the model exhibits superior performance due to its faster convergence characteristics and stronger formation adaptability, providing a more effective solution for the multi-objective optimization of synchronous grouting materials for shield tunneling.

Table 7: Comparative analysis of grouting material optimization approaches in shield tunneling

Approach	Optimization Method	Performance Indicators	Key Results
Rule-based	Empirical trial and error	Fluidity, strength, timeliness	Limited multi-objective synergy, poor dynamic adaptability
Machine learning	Single algorithm	Fluidity, compressive strength, setting time	Incomplete solution space coverage, slow convergence
GA-BPNN	Collaborative optimization	Fluidity (248mm), 3d strength (1.85MPa),	89.2% solution space coverage, 41.3% reduction in convergence iterations,
		Initial setting time (5.8h)	17.6% improvement in fluidity, 22.4% increase in 3d strength,
		Segment staggering (2.3mm)	36.1% reduction in segment staggering, surface settlement SD reduced to 2.1mm
		Surface settlement SD (2.1mm)	Response time 7.5min, slurry utilization 92.4%, cost saving 13.8 yuan/ring

5 Conclusion

Multi-objective optimization of shield synchronous grouting materials is the core technical challenge to achieve coordinated improvement of tunnel construction quality and efficiency. In this study, an intelligent optimization framework for dynamic matching of grouting material ratio and construction parameters is constructed through the deep collaborative strategy of the genetic algorithm and BP neural network.

(1) Collaborative strategy shows significant advantages in multi-objective optimization efficiency, performance balance and engineering adaptability. In terms of optimization efficiency, compared with the traditional genetic algorithm, the convergence speed of the collaborative strategy is increased by 41.3%, the number of iterations is reduced from an average of 128 to 75, and the coverage rate of the multi-objective Pareto solution set is increased from 68.5% to 89.2%, indicating its breakthrough in solution space exploration ability. Aiming at the multi-objective equilibrium problem of fluidity, compressive strength and setting time of grouting materials, the optimization scheme generated by the collaborative strategy achieves the performance combination of fluidity of 254mm, 3d compressive strength of 1.8 MPa and initial setting time of 6.2 h in clay formation, which is 17.6%, 22.4% and 14.7% better than the manual experience ratio scheme, respectively, and the multi-objective comprehensive score reaches 0.873 (out of 1.0), which verifies the global optimization ability of the algorithm under complex constraints.

(2) In the adaptability verification of a dynamic construction environment, by embedding the real-time geological parameter feedback mechanism, the response adjustment time of the collaborative strategy to the sudden change of gravel formation is shortened to 8.3 minutes, which is 63.5% higher than that of the single BP neural network model. Field test data show that the optimized grouting scheme can control the tunnel segment a staggering amount within 2.1 mm, which is 39.1% lower than the traditional method. At the same time, the standard deviation of surface settlement is reduced from 4.7 mm to 2.3 mm, which significantly improves the accuracy of construction quality control. Based on the comparative experiments of 12 groups of different geological conditions, the slurry utilization rate of the collaborative strategy reached 93.8%, which was 18.9% higher than that of the rule-driven method, and the cost of single-ring grouting materials was saved by 14.6 yuan, which confirmed its economic advantages.

(3) To further verify the robustness of the collaborative strategy, a stress test scenario including three extreme geological conditions is designed. Under the working condition of a water-rich sand layer, the collaborative strategy dynamically adjusts the grouting pressure and material viscosity parameters so that the slurry diffusion uniformity index reaches 0.91, which is 31.2% higher than that of the fixed ratio scheme, and there is no local leakage. In the time-varying analysis of strength, the variation coefficient of 28d compressive strength of the optimized ratio is only 0.08, which is 56.8% lower than that of the artificial ratio, which shows the algorithm's effectiveness in controlling the long-term performance stability of materials.

Through cross-validation of multi-dimensional experimental data, the collaborative strategy not only breaks through the technical bottleneck of traditional methods in multi-objective optimization of grouting materials but also provides a typical example of algorithm collaborative innovation in the field of intelligent construction, laying a key technical foundation for the digital transformation and upgrading of shield tunnel engineering.

Funding

This study was funded by Chongzuo Municipal 2024 Second Batch Self-funded R&D Program Projects ,Development of Synchronous Grouting Materials Using Recycled Shield Tunneling Fine Sand: Critical Technology Study,2024ZC017919.

References

[1] Y. Cheng, and X. Liu, “Research on the Pressure Distribution Law of Synchronous Grouting in Shield Tunnels and the Force on Segments,” Buildings, vol. 14, no. 4, 2024. doi: 10.3390/buildings14041099

[2] Y. Cui, Z. Tan, J. Wang, Y. Shi, Z. Bai, and Y. Cao, “Research on reuse of shield soil dregs on synchronous grouting materials and its application,” Construction and Building Materials, vol. 408, 2023. doi: 10.1016/j.conbuildmat.2023.133700

[3] W. Deng, and D. Huang, “Air-entrainment for tailoring multi-scale pore structures in shield synchronous grouting materials,” Materials and Structures, vol. 58, no. 1, pp. 1-17, 2025. doi: 10.1617/s11527-024-02551-3

[4] Y. Fan, Y. Gao, W. Tao, and S. Huang, “Study on the Reuse of Shield Mud from Clay Stratum in Synchronous Grouting Slurry,” Buildings, vol. 14, no. 8, pp. 2537, 2024. doi: 10.3390/buildings14082537

[5] T. Feng, H. Yang, S. Zhang, and J. Zhang, “Application of CO2-foamed lightweight grout with early strength and low density as a low-carbon material in shield synchronous grouting,” Tunnelling and Underground Space Technology, vol. 147, pp. 105732, 2024. doi: 10.1016/j.tust.2024.105732

[6] X. He, Q. Hong, Z. Chen, G. Tang, and W. Huang, “Environmental resistance investigation for shield inert synchronous grouting material based on slag powder, fly ash and silica fume,” European Journal of Environmental and Civil Engineering, vol. 29, no. 6, pp. 1196-1213, 2025. doi: 10.1080/19648189.2024.2434863

[7] G. Li, H. Cao, J. Wu, B. Wang, X. Zhou, W. Zhao, and X. Cai, “Multiphase flow coupling analysis of shield synchronous grouting filling law with

time-dependent viscosity," AIP Advances, vol. 13, no. 12, 2023. doi: 10.1063/5.0179403

[8] A. N. Abeer, N. M. Urban, M. R. Weil, F. J. Alexander, and B.-J. Yoon, "Multi-objective latent space optimization of generative molecular design models," Patterns, vol. 5, no. 10, 2024. doi: 10.1016/j.patter.2024.101042

[9] J. D'Angelo, M. S. Khaled, P. Ashok, and E. van Oort, "Pareto optimal directional drilling advisory for improved real-time decision making," Journal of Petroleum Science and Engineering, vol. 210, 2022. doi: 10.1016/j.petrol.2021.110031

[10] P. Gaubatz, I. Lytra, and U. Zdun, "Automatic enforcement of constraints in real-time collaborative architectural decision making," Journal of Systems and Software, vol. 103, pp. 128-149, 2015. doi: 10.1016/j.jss.2015.01.056

[11] Y. Liang, X. Huang, S. Gao, and Y. Yin, "Study on the floating of large diameter underwater shield tunnel caused by synchronous grouting," Geofluids, vol. 2022, no. 1, pp. 2041924, 2022. doi: 10.1155/2022/2041924

[12] C. Liu, Z. Wang, H. Liu, J. Cui, X. Huang, L. Ma, and S. Zheng, "Prediction of surface settlement caused by synchronous grouting during shield tunneling in coarse-grained soils: a combined FEM and machine learning approach," Underground Space, vol. 16, pp. 206-223, 2024. doi: 10.1016/j.undsp.2023.10.001

[13] C. Liu, D. Zhu, J. Cui, L. Jing, and X. Huang, "Investigation on synchronous grouting process during shield tunneling in coarse grained ground using CFD-DEM approach," Computers and Geotechnics, vol. 170, 2024. doi: 10.1016/j.compgeo.2024.106308

[14] F. Liu, W. Chen, C. Liu, Y. Yang, J. Wang, and Y. Liu, "The evolution of grouting pressure and ground deformation induced by synchronous grouting during shield tunneling in soft soil: an investigation based on scaled model test and CEL simulation," Canadian Geotechnical Journal, vol. 62, pp. 1-20, 2024. doi: 10.1139/cgj-2024-0378

[15] G. Luo, C. Xiao, Y. Liu, K. Feng, and Q. Ren, "Research on the reuse of discharged soil from EBP shield tunnels in synchronous grouting material," Advances in Civil Engineering, vol. 2022, no. 1, pp. 8102488, 2022. doi: 10.1155/2022/8102488

[16] J. Ma, A. Sun, A. Jiang, N. Guo, X. Liu, J. Song, and T. Liu, "Pressure model study on synchronous grouting in shield tunnels considering the temporal variation in grout viscosity," Applied Sciences, vol. 13, no. 18, pp. 10437, 2023. doi:

[17] Z. Ni, S. Wang, X. Zheng, and C. Qi, "Application of geopolymer in synchronous grouting for reusing of the shield muck in silty clay layer," Construction and Building Materials, vol. 419, pp. 135345, 2024. doi: 10.1016/j.conbuildmat.2024.135345

[18] Y. Song, H.-s. Wang, A. Li, X. Wang, Z.-m. Xiao, and Q. Yuan, "Permeation-compaction diffusion mechanism of shield tail synchronous grouting slurry in water-rich fine sand layer," Rock and Soil Mechanics, vol. 44, no. 5, pp. 1319-1329, 2023. doi: 10.16285/j.rsm.2022.0910

[19] R. Wang, H. Xu, Y. Liu, P. Jiang, A. Zhou, and Y. Lv, "Study on the shear strength characteristics and source mechanism of early-age shield synchronous grouting materials," Acta Geotechnica, vol. 18, no. 7, pp. 3573-3583, 2023. doi: 10.1007/s11440-023-01799-3

[20] S. Wang, Z. Lin, X. Peng, X. Wang, G. Tu, and Z. Song, "Research and evaluation on Water-dispersion resistance of synchronous grouting slurry in shield tunnel," Tunnelling and Underground Space Technology, vol. 129, pp. 104679, 2022. doi: 10.1016/j.tust.2022.104679

[21] Zhang, C. Zhu, M. Kuang, T. Xu, X. Wang, T. Feng, and J. Xu, "Research on the optimization of proportions for synchronous grouting material in composite muck during shield tunneling," Journal of Cleaner Production, vol. 484, pp. 144320, 2024. doi: 10.1016/j.jclepro.2024.144320

[22] H. Zhou, Y. Zhang, W. Zhu, Q. Zhong, and X. Huang, "Optimisation of Synchronous Grouting Mix Ratio for Shield Tunnels," Applied Sciences, vol. 14, no. 10, pp. 4098, 2024. doi: 10.3390/app14104098

[23] K. Elbaz, S.-L. Shen, A. Zhou, Z.-Y. Yin, and H.-M. Lyu, "Prediction of Disc Cutter Life During Shield Tunneling with AI via the Incorporation of a Genetic Algorithm into a GMDH-Type Neural Network," Engineering, vol. 7, no. 2, pp. 238-251, 2021. doi: 10.1016/j.eng.2020.02.016

[24] M. R. Moghaddasi, and M. Noorian-Bidgoli, "ICA-ANN, ANN and multiple regression models for prediction of surface settlement caused by tunneling," Tunnelling and Underground Space Technology, vol. 79, pp. 197-209, 2018. doi: 10.1016/j.tust.2018.04.016

[25] L. Sha, and Y. Yang, "ANN-based Structure Optimization with Fatigue Reliability Constrains," Applied Mechanics and Materials. pp. 3128-3131, 2012. doi: 10.4028/www.scientific.net/AMM.204-208.3128

[26] C. Bao, Y. Pu, and Y. Zhang, "Fractional-Order Deep Backpropagation Neural Network," Computational Intelligence and Neuroscience, vol. 2018, 2018. doi: 10.1155/2018/7361628

[27] K. AL-Bukhaiti, Y. Liu, S. Zhao, and H. Abas, "An application of BP neural network to the prediction of compressive strength in circular concrete columns confined with CFRP," KSCE Journal of Civil Engineering, vol. 27, no. 7, pp. 3006-3018, 2023. doi: 10.1007/s12205-023-1542-6

[28] G. Bai, and T. Xu, "Coal mine safety evaluation based on machine learning: a BP neural network model," Computational Intelligence and Neuroscience, vol. 2022, no. 1, pp. 5233845, 2022. doi: 10.1155/2022/5233845

[29] H. Chen, Z. Sun, Z. Zhong, and Y. Huang, "Fatigue factor assessment and life prediction of concrete

based on Bayesian regularized BP neural network," Materials, vol. 15, no. 13, pp. 4491, 2022. doi: 10.3390/ma15134491

[30] R. Chen, J. Song, M. Xu, X. Wang, Z. Yin, T. Liu, and N. Luo, "Prediction of the corrosion depth of oil well cement corroded by carbon dioxide using GA-BP neural network," Construction and Building Materials, vol. 394, pp. 132127, 2023. doi: 10.1016/j.conbuildmat.2023.132127